Proc. Natl. Acad. Sci. USA
Vol. 86, pp. 6944–6948, September 1989
Biochemistry

Melittin binding causes a large calcium-dependent conformational change in calmodulin

(solution structure/small-angle x-ray scattering/calcium regulation)

MIKIO KATAOKA*, JAMES F. HEAD†, BARBARA A. SEATON†, AND DONALD M. ENGELMAN*

*Department of Molecular Biophysics and Biochemistry, Yale University, New Haven, CT 06511; and †Department of Physiology, Boston University School of Medicine, Boston, MA 02118-2394

Communicated by Frederic M. Richards, June 26, 1989 (received for review May 3, 1989)

ABSTRACT **The interaction between calmodulin and its target protein is a key step in many calcium-regulated cellular functions. Melittin binds tightly to calmodulin in the presence of calcium and is a competitive inhibitor of calmodulin function. Using melittin as a model for the target peptide of calmodulin, we have found a large Ca^{2+}-dependent conformational change of calmodulin in solution induced by peptide binding. Mg^{2+} does not substitute for Ca^{2+} in producing the conformation change. Small-angle x-ray scattering has shown that calmodulin exists as a dumbbell in solution, similar to that observed in the crystalline state. Our present measurements reveal that the overall structure of the Ca^{2+}–calmodulin–melittin complex is not a dumbbell but a globular shape. Upon binding melittin, the radius of gyration decreases from 20.9 to 18.0 Å and the largest dimension decreases from 60 to 47.5 Å. In the absence of calcium, however, melittin has little effect on the solution structure of calmodulin.**

The principal means by which cells respond to the increases in intracellular free calcium ion concentration produced by primary stimuli is through calcium receptor proteins. These proteins act as "molecular switches" in various biochemical pathways by binding calcium ions reversibly and by altering their interaction with target proteins. Such interactions activate the protein targets, stimulating physiological processes in response to the calcium signal. Calmodulin is the most extensively studied intracellular calcium-binding protein, both in terms of its structure and with respect to its role in modulating a variety of cell functions through its interactions with many different enzymes (for review, see ref. 1).

Because of the importance of calmodulin–enzyme interactions, much work has focused on the molecular mechanisms underlying the protein–protein interaction and the ensuing enzyme activation. The crystal structure of calmodulin (2–4) has provided the structural framework for numerous studies. In crystals, calmodulin and its close homologue troponin C adopt an unusual dumbbell shape (2–6). The two lobes of the dumbbell are connected by a central helix. Because of its unusual shape and high surface/volume ratio, this structure has raised many questions related to the form and function of the protein, including the relationship between the crystal and solution structures and the possibility of alternative conformations. Some of these questions have been addressed through techniques such as small-angle x-ray scattering (7, 8). From small-angle x-ray scattering data, information about molecular size and shape can be obtained from protein molecules in solution, thus providing complementary data to those obtained from crystallographic methods. While small-angle x-ray scattering is a much lower resolution technique than x-ray crystallography, a major advantage, in addition to the ability to measure proteins in solution, is that samples can be studied under near-physiological conditions, which is frequently impossible for protein crystals.

Differences between solution and crystal structures of calmodulin seem most likely to involve dynamic aspects of the spatial relationship of the two lobes of the molecule, governed by flexibility of the central helical region. Previous small-angle x-ray scattering studies on calmodulin (7, 8) have indicated that in solution the protein possesses an elongated bilobed shape, generally consistent with the crystal structure. However, such measurements provide information only on the time-averaged structure and do not preclude the possibility that flexibility in the helix may exist. The consequences of such flexibility, particularly in terms of its role in the interactions of calmodulin with its target proteins, have been discussed (8–10). Persechini and Kretsinger (9) have proposed that the central helix serves as a "flexible tether" permitting the lobes to wrap around the calmodulin-binding region of the target. Because of the large size and complexity of most of the target proteins of calmodulin, it has proved difficult to approach this issue directly by structural study of a calmodulin–enzyme complex. However, several calmodulin-binding peptides have been identified, including the bee venom peptides melittin and mastoparan as well as the peptide that is believed to represent the calmodulin binding region of myosin light-chain kinase. These peptides bind to calmodulin in a calcium-dependent manner with high affinity and are believed to mimic the binding between calmodulin and its native targets (11–13).

In this paper, we extend our earlier small-angle x-ray scattering studies on calmodulin to include considerations of the effects of the binding of one of these peptides, melittin, on the structure of the protein. Since NMR studies show that binding of the major physiological intracellular divalent cation magnesium also alters the structure of calmodulin (14), we have included considerations of the effects of this ion on the protein in the presence and absence of melittin.

EXPERIMENTAL PROCEDURES

Protein Preparations. Bovine brain calmodulin was prepared by the method of Masure *et al.* (15). The bee venom peptide melittin was purchased from Sigma and repurified by HPLC before use. HPLC was performed with an ISCO 2360 gradient maker, model 2350 pump, and model V4 detector measuring absorption at 280 nm. Approximately 5 mg of melittin dissolved in 250 μl of 0.1% trifluoroacetic acid was loaded onto a Vydac C-18 column (4 × 250 mm) and eluted with a linear 45–50% gradient of acetonitrile in 0.1% trifluoroacetic acid over 20 min at a flow rate of 1 ml/min. Melittin eluted as a single major peak, resolved from several minor contaminants. The fractions containing purified melittin were pooled and dried in a Savant Speedvac concentrator. The purification was repeated several times to accumulate sufficient pure melittin for the studies described.

The publication costs of this article were defrayed in part by page charge payment. This article must therefore be hereby marked "*advertisement*" in accordance with 18 U.S.C. §1734 solely to indicate this fact.

Sample Preparation. Stock solutions of calmodulin and melittin were prepared by dissolving freeze-dried protein in water. The concentrations of the stock solutions were determined by quantitative amino acid analysis. Samples of calmodulin alone or calmodulin mixed in equimolar amounts with the stock melittin solution were dialyzed against one of the solutions described below. Samples were dialyzed at a concentration of 20–50 mg/ml in Spectra/por 4 dialysis membrane (molecular weight cut-off, 12,000–14,000), which had been prepared for use as described (16). Dialyses of 0.2- to 0.5-ml samples were performed at 4°C against three changes of 100 ml of the described solutions, the first two changes being after 24 hr each and the final dialysis being for 72 hr to ensure complete equilibration. At the end of this time, the samples were removed from the dialysis tubing and aliquots were quantitatively diluted with the final dialysis fluid to produce a concentration series ranging from ≈5 mg/ml to up to 50 mg/ml. The protein concentrations of the dialyzed samples were also determined, again by quantitative amino acid analysis, to permit calculation of accurate concentrations for the members of the dilution series.

Dialysis solutions all contained 100 mM KCl, 50 mM Mops, 0.02% sodium azide (pH 7.4). For samples in the presence of calcium, the initial dialysis fluid included an additional 1 mM $CaCl_2$ to ensure saturation of Ca^{2+}-binding sites; the subsequent two changes of dialysis fluid each contained 0.1 mM $CaCl_2$. For samples in the absence of calcium (pCa < 8), the initial dialysis fluid contained 5 mM EGTA and subsequent changes contained 1 mM EGTA. For samples containing magnesium, the dialysis fluid included 3 mM $MgCl_2$. For dialyses of samples containing melittin, the dialysis fluid also included 1 μM melittin. Test experiments showed that no melittin is lost during dialysis.

Small-Angle X-Ray Scattering Measurements. X-rays (λ, 1.54 Å) generated by an Elliott GX-6 rotating anode generator were focused using two 20-cm-long glass mirrors. Two 4-jawed slits were used to restrict parasitic scattering: one was placed just after the second mirror and the other was placed in front of the specimen cell. Upstream of the specimen chamber, the beam path was filled with He. The path between specimen and detector was evacuated to avoid air scattering. Scattering profiles were recorded by a linear position-sensitive detector connected to a Canberra multichannel analyzer. The uniformity of the detector was occasionally checked and data were corrected if necessary. The specimen-to-detector distance was either 50 cm or 62 cm, and it was calibrated by using the powder pattern of cholesteryl myristate. Exposure times were between 1 and 6 hr. A series of measurements with different protein concentrations was performed with a fixed exposure time. Sample temperature was kept at 20°C during exposure. The backward scatter from the lead beam stop was monitored during the exposure to normalize each set of scattering data for source fluctuations and sample transmission. The final dialysis buffer of each preparation was also measured as the background.

Data Analysis. Scattering data were stored in a multichannel analyzer and transferred to a VAX 8800. A scattering curve at infinite dilution was obtained by separate extrapolation of each point in reciprocal space from a set of scattering curves at different protein concentrations. The extrapolated curve was analyzed by Guinier analysis (17), the indirect Fourier transform analysis of Moore (18), and the domain analysis developed by Fujisawa *et al.* (19). For the Guinier analysis, data were used to $Q = 0.09$ Å^{-1} for every data set except for that of the Ca^{2+}–calmodulin–melitten complex, where data were included to $Q = 0.15$ Å^{-1} ($Q = 4\pi \sin\theta/\lambda$; 2θ = scattering angle; λ = x-ray wavelength). The innermost measured scattering point is at $Q = 0.02$ Å^{-1}. Scattering data up to $Q = 0.3$ Å^{-1} were used to calculate the distance distribution function, $p(r)$, by the indirect Fourier transform. The distance between two lobes was estimated by the following relationship:

$$Rg^2 = Rd^2 + d^2/4,$$

where Rg, Rd, and d are the radius of gyration of a whole molecule (solute), the average radius of gyration of each lobe, and the distance between the two lobes, respectively.

RESULTS

A conformational change of Ca^{2+}–calmodulin upon binding of melittin is clearly evident in the small-angle x-ray scattering curves. Fig. 1*a* shows Guinier plots of both Ca^{2+}–calmodulin and the Ca^{2+}–calmodulin–melittin complex within the Guinier region. Fig. 1*b* shows the extended scattering curve in the form of a Guinier plot. There are significant changes in the scattering curve upon binding of melittin.

First, the scattered intensity at zero angle, $I(0)$, increased (Fig. 1*a*). This observation is expected from the increase of the molecular weight of the solute, consistent with formation of a 1:1 calmodulin–melittin complex. The observed $I(0)$ values for calmodulin and the calmodulin–melittin complex were 80.0 ± 0.8 and 89.0 ± 1.1, respectively. Using staphylococcal nuclease as a standard [$I(0)$ = 75.5 ± 0.5; M_r, 16,808], the estimated molecular weight increase is 2000 ± 300, which is comparable to the molecular weight of melittin, 2800.

Second, the radius of gyration is dramatically decreased after formation of the complex, which is seen from the decrease of the slope in Fig. 1*a*. The structural parameters

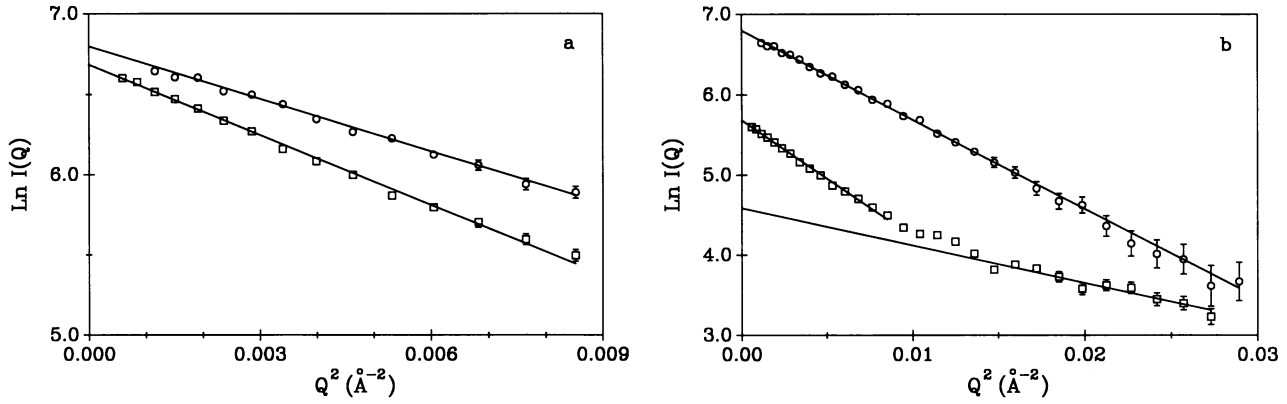

FIG. 1. Guinier plot of calmodulin (□) and calmodulin–melittin complex (○) in the presence of both Ca^{2+} and Mg^{2+}. (*a*) Guinier region. (*b*) Guinier region including higher scattering angle region. For clarity, the values for calmodulin without melittin in *b* are shifted by −1 unit on the ln *I* axis.

obtained are summarized in Table 1. Melittin is known to form an α-helix when it binds to calmodulin (20). The expected radius of gyration of an α-helical melittin monomer is around 13 Å. If the conformation of calmodulin is not changed by the binding of melittin, then the radius of gyration of the complex should be increased. Thus, the observed decrease strongly suggests a large conformational change of calmodulin.

Third, the shape of the scattering curve of Ca^{2+}–calmodulin changes considerably with complex formation (Fig. 1*b*). The Guinier plot for Ca^{2+}–calmodulin alone in solution shows two distinct regions where the plots can be approximated by straight lines. The innermost straight line region is the so-called Guinier region for calmodulin, from which the radius of gyration can be obtained. This region has been analyzed and characterized (7, 8). The existence of the second straight line region is characteristic for a dumbbell-shaped structure. Fujisawa *et al.* (19) indicated that the average radius of gyration of the two globular domains of a dumbbell can be estimated from this region using a $\ln(I(Q)/Q)$ vs. Q^2 plot. The Guinier plot of Ca^{2+}–calmodulin clearly suggests that calmodulin exists as a dumbbell structure in solution. On the other hand, for the Ca^{2+}–calmodulin–melittin complex, the Guinier plot shows only a single straight line, corresponding to the Guinier region, which is typical for globular proteins. The disappearance of the second straight line region in the plot again suggests a large conformational change in calmodulin on binding melittin. It is likely that the structural transition is from a dumbbell shape to a globular shape.

The dumbbell-to-globular structural transition is confirmed by the $p(r)$ function shown in Fig. 2. The $p(r)$ function of Ca^{2+}–calmodulin is consistent with a dumbbell structure; one major peak around 20 Å is interpreted as the distribution of intradomain vectors and a shoulder near 45 Å is due to the distribution of interdomain vectors (7, 8). The maximum dimension of Ca^{2+}–calmodulin is estimated to be 60.0 Å. In contrast, the $p(r)$ function of the complex shows only one maximum, which is as expected for a globular molecule. The maximum dimension of the complex is 47.5 Å. Thus, the structural parameters, the scattering profile, and the $p(r)$ function all indicate a large conformational change of calmodulin upon binding of melittin in the presence of Ca^{2+}.

The melittin-induced conformational change in calmodulin is dependent on Ca^{2+}. Fig. 3 shows Guinier plots of calmodulin solutions with and without melittin in the absence of Ca^{2+}. The two linear regions are clearly seen for EGTA–calmodulin both with and without melittin, suggesting that calmodulin has a dumbbell shape under both conditions. However, both $I(0)$ and the radius of gyration increase for EGTA–calmodulin with melittin. The most likely explanation for these changes is the formation of a low-affinity complex between calmodulin and melittin in the absence of Ca^{2+}, which does not give rise to the dumbbell to globular structural transition in the calmodulin molecule. The formation of a low-affinity complex in the absence of calcium has been reported previously (21).

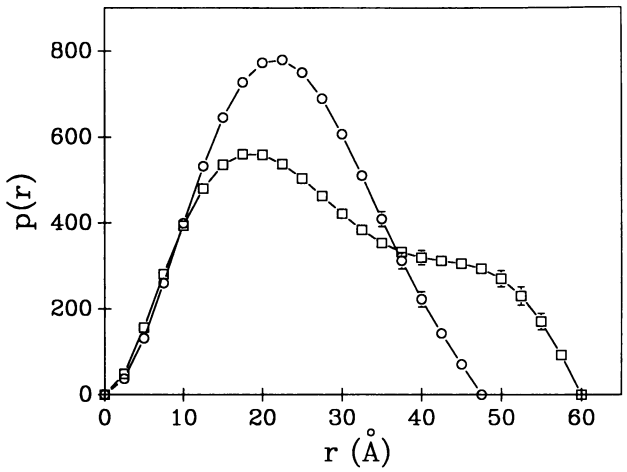

FIG. 2. Comparison of distance distribution function, $p(r)$, for calmodulin with that for calmodulin–melittin complex in the presence of Ca^{2+}. □, Ca^{2+}–calmodulin; ○, Ca^{2+}–calmodulin–melittin complex.

Each measurement described above was carried out in the presence or absence of Mg^{2+}, whereas previous scattering experiments on calmodulin in solution have been performed in the absence of Mg^{2+} (7, 8). Magnesium is known to compete with calcium for binding sites on calmodulin (14). Our studies show that in the absence of Ca^{2+}, Mg^{2+} has a small but distinct effect on unliganded calmodulin. As is shown in Table 1, Mg^{2+} causes a decrease both in the radius of gyration and in the maximum dimension of the protein. These decreases can be attributed to a slight shrinkage of each domain without a shortening of the distance between them.

The binding of Ca^{2+} to calmodulin, on the other hand, produces an increase in both the radius of gyration and the

Table 1. Structural parameters determined by small-angle x-ray scattering

Condition	*Rg* (Guinier),* Å	*Rg* (Moore),† Å	*Rg* (domain),‡ Å	d_{max},§ Å	*D*,¶ Å
+ Mg^{2+}					
− Melittin					
− Ca^{2+}	19.04 (0.07)	19.87 (0.06)	14.4 (0.2)	55.0	27.2 (0.6)
+ Ca^{2+}	20.91 (0.20)	22.06 (0.21)	14.7 (0.9)	60.0	32.9 (2.2)
+ Melittin					
− Ca^{2+}	20.40 (0.24)	21.14 (0.23)	16.3 (1.0)	57.5	29.7 (2.9)
+ Ca^{2+}	17.96 (0.24)	17.61 (0.14)	—	47.5	—
− Mg^{2+}					
− Melittin					
− Ca^{2+}	19.46 (0.11)	20.33 (0.11)	15.0 (0.2)	57.5	27.4 (0.8)
+ Ca^{2+}	20.17 (0.16)	22.58 (0.27)	14.7 (0.6)	62.5	34.3 (1.7)
+ Melittin					
− Ca^{2+}	20.90 (0.22)	22.54 (0.20)	17.1 (1.3)	60.0	29.4 (3.6)
+ Ca^{2+}	18.01 (0.15)	17.85 (0.13)	—	47.5	—

*The radius of gyration of the molecule obtained by Guinier analysis.
†The radius of gyration of the molecule obtained by Moore analysis.
‡The average radius of gyration of each domain obtained by the domain analysis.
§The maximum dimension of the molecule estimated from $p(r)$ function.
¶The distance between two domains calculated with use of *Rg* (Moore) and *Rg* (domain).

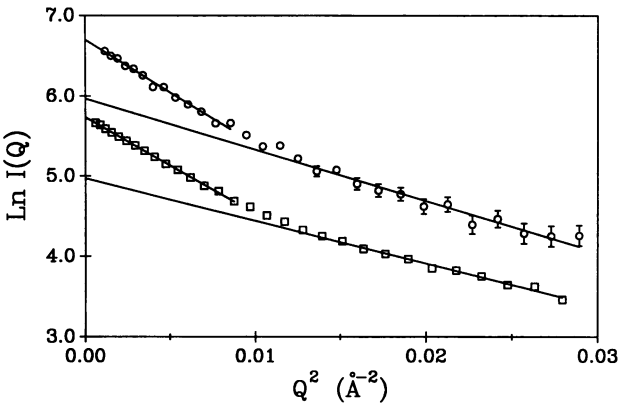

FIG. 3. Guinier plot of calmodulin in the absence of Ca^{2+} without melittin (□) and with melittin (○). For clarity, the values for calmodulin without melittin are shifted by −1 unit on the ln *I* axis.

maximum dimension of the protein. Domain analysis suggests that these changes result from an increase in the distance between the two domains without significant alterations in the size of each domain (Table 1). In the presence of Ca^{2+}, Mg^{2+} has little effect on calmodulin structure, particularly with respect to melittin binding: the large conformational change associated with peptide binding is Ca^{2+} specific.

DISCUSSION

Small-angle x-ray scattering has revealed that the dumbbell shape of calmodulin is changed to a globular shape upon binding melittin in the presence of Ca^{2+}. This fact indicates that the central helix is highly flexible, as has been previously suggested (8–10). The decreases of both radius of gyration and maximum distance can be interpreted as a hinge motion of the central helix bringing the lobes of calmodulin in contact, perhaps binding melittin in between, which is similar to the model proposed by Persechini and Kretsinger (10). The maximum length of their model, however, is significantly larger than the value we observe. This suggests that the conformational change that occurs may be even more extreme than that suggested by the model derived using their constraints (10).

Calmodulin–peptide complexes have been investigated by various techniques (12, 20–26). Most of these studies describe a conformational change of the bound peptide. Melittin adopts an α-helical form when it binds to calmodulin, while it generally exists as a coil in solution (20). Although some authors have pointed out the possibility of a conformational change in calmodulin on complex formation, the magnitude and nature of the change have not been characterized (20, 24, 26).

Cox *et al.* (25) observed that the circular dichroism spectrum of the complex differs from that of calmodulin itself and that the change can be ascribed to a conformational change in the peptide. Their observation suggests that secondary structure changes in calmodulin upon binding of melittin are, if any, small. On the other hand, Klevit *et al.* (24) reported the possibility of a secondary structural change in calmodulin on complex formation as well as a tertiary structural change.

X-ray solution scattering profiles extending beyond the Guinier region contain information regarding the shape and internal structure of proteins (27). The solution scattering profile of Ca^{2+}–calmodulin gave two broad maxima in the Q region between 0.25 $Å^{-1}$ and 0.65 $Å^{-1}$, which is expected from predictions based on the crystal structure. The profile between Q = 0.25 $Å^{-1}$ and 0.5 $Å^{-1}$ was clearly changed by binding of melittin, while the maximum around Q = 0.6 $Å^{-1}$ remained the same (M.K., J. Flanagan, and D.M.E., unpublished results). The latter maximum is a characteristic of α-helical proteins and is interpreted as the interaction of two adjacent helices (28). These preliminary experiments suggest that the structural rearrangement occurs without significant alteration of the proportion of types of secondary structure.

Although melittin binds tightly to calmodulin in the presence of Ca^{2+}, it is unlikely to be a physiological target protein. However, melittin appears to competitively inhibit the binding of a target enzyme to calmodulin (11), suggesting that the binding site may be the same. Thus, we can regard melittin as a model of the calmodulin binding region of a target enzyme. Recently, two other groups have independently investigated conformational changes of calmodulin upon binding peptides, using small-angle x-ray scattering and neutron scattering (29–31). One used mastoparan as a model peptide (29) and the other used a synthetic peptide corresponding to what is believed to be the calmodulin binding site of myosin light-chain kinase (30, 31). Both observed the same phenomenon as described in the present study, although the exact values of structural parameters differ slightly from each other, possibly as a consequence of the differences in the sizes of the peptides.

The existence of a large, peptide-, and calcium-dependent conformational change in calmodulin is now established by parallel and independent work in three laboratories using three different peptides (29–31). It seems reasonable to expect that the changes may be a general feature of the calmodulin-mediated calcium-activation mechanism.

We wish to express our sincere gratitude to P. Moore and J. Flanagan for valuable discussions, to R. Kretsinger for sending us a preprint of their model, to H. Yoshino for showing us his unpublished data on calmodulin–mastoparan complex, to J. Trewhella for discussions, to G. Johnson for skillful technical assistance. This work was supported by National Institutes of Health Grants GM 22778 (D.M.E.) and NS 20357 (J.F.H.), and by National Science Foundation Grant DMB-9910355 (B.A.S.). B.A.S. is the recipient of an American Cancer Society Junior Faculty Research Award (JFRA-215).

1. Klee, C. B. & Vanaman, T. C. (1982) *Adv. Protein Chem.* **35,** 213–321.
2. Babu, Y. S., Sack, J. S., Greenhough, T. J., Bugg, C. E., Means, A. R. & Cook, W. J. (1985) *Nature (London)* **315,** 37–40.
3. Kretsinger, R. H., Rudnick, S. E. & Weissman, L. J. (1986) *J. Inorg. Biochem.* **28,** 289–302.
4. Babu, Y. S., Bugg, C. E. & Cook, W. J. (1988) *J. Mol. Biol.* **204,** 191–204.
5. Herzberg, O. & James, M. N. G. (1985) *Nature (London)* **313,** 653–659.
6. Sundaralingam, M., Bergstrom, R., Strasburg, G., Rao, S. T., Roychowdhury, P., Greaser, M. & Wang, B. C. (1985) *Science* **227,** 945–948.
7. Seaton, B. A., Head, J. F., Engelman, D. M. & Richards, F. M. (1985) *Biochemistry* **24,** 6740–6743.
8. Heidorn, D. B. & Trewhella, J. (1988) *Biochemistry* **27,** 909–915.
9. Persechini, A. & Kretsinger, R. H. (1988) *J. Biol. Chem.* **263,** 12175–12178.
10. Persechini, A. & Kretsinger, R. H. (1988) *J. Cardiovasc. Pharmacol.* **12** (Suppl. 5), S1–S12.
11. Comte, M., Maulet, Y. & Cox, J. A. (1983) *Biochem. J.* **209,** 269–272.
12. Malencik, D. A. & Anderson, S. R. (1984) *Biochemistry* **23,** 2420–2428.
13. Blumenthal, D. K., Takio, K., Edelman, A. M., Charbonneau, H., Titani, K., Walsh, K. A. & Krebs, E. G. (1985) *Proc. Natl. Acad. Sci. USA* **82,** 3187–3191.
14. Tsai, M.-D., Drakenberg, T., Thulin, E. & Forsen, S. (1987) *Biochemistry* **26,** 3635–3643.
15. Masure, H. R., Head, J. F. & Tice, H. (1984) *Biochem. J.* **218,** 691–696.

16. Sheldon, A. & Head, J. F. (1988) *J. Biol. Chem.* **263,** 14384–14389.
17. Guinier, A. & Fournet, G. (1955) *Small-Angle Scattering of X-Rays* (Wiley, New York).
18. Moore, P. B. (1980) *J. Appl. Crystallogr.* **13,** 168–175.
19. Fujisawa, T., Ueki, T., Inoko, Y. & Kataoka, M. (1987) *J. Appl. Crystallogr.* **20,** 349–355.
20. Seeholzer, S. H., Cohn, M., Putkey, J. A., Means, A. R. & Crespi, H. L. (1986) *Proc. Natl. Acad. Sci. USA* **83,** 3634–3638.
21. Maulet, Y. & Cox, J. A. (1983) *Biochemistry* **22,** 5680–5686.
22. Malencik, D. A. & Anderson, S. R. (1982) *Biochemistry* **21,** 3480–3486.
23. O'Neil, K. T., Wolfe, H. R., Jr., Erickson-Viitanen, S. & DeGrado, W. F. (1987) *Science* **236,** 1454–1456.
24. Klevit, R. E., Blumenthal, D. K., Wemmer, D. E. & Krebs, E. G. (1985) *Biochemistry* **24,** 8152–8157.
25. Cox, J. A., Comte, M., Fitton, J. E. & DeGrado, W. F. (1985) *J. Biol. Chem.* **260,** 2527–2534.
26. Yazawa, M., Ikura, M., Hikichi, K., Ying, L. & Yagi, K. (1987) *J. Biol. Chem.* **262,** 10951–10954.
27. Pickover, C. A. & Engelman, D. M. (1982) *Biopolymers* **21,** 817–831.
28. Vainshtein, B. K. (1966) *Diffraction of X-Rays by Chain Molecules* (Elsevier, Amsterdam), pp. 164–172.
29. Matsushima, N., Izumi, Y., Matsuo, T., Yoshino, H., Ueki, T. & Miyake, Y. (1989) *J. Biochem (Tokyo)* **105,** 883–887.
30. Heidorn, D. B., Rokop, S. E., Seeger, P. A., Blumenthal, D. K., Means, A. R., Crespi, H. & Trewhella, J. (1989) *Biophys. J.* **55,** 528a (abstr.).
31. Heidorn, D. B., Rokop, S. E., Seeger, P. A., Blumenthal, D. K., Means, A. R., Crespi, H. & Trewhella, J. (1989) *Biochemistry*, in press.